tion of the form $(2l+1)e^{-l/10}$ was necessary. No reason for this behavior was proffered and, subsequently, Ponomarev[9] has suggested that such a violent change in the initial l distribution, for nearby elements, seems unnatural. From the point of view of atomic dimensions, however, this is precisely the expectation, since the atomic diameters of Ti and Mn are 2.93 and 2.5 Å, respectively. Thus, we would expect a truncation in l for the initial angular distribution in Mn which would be reflected later in the cascade by a diminished circular orbit population for Mn as compared to Ti.

It may be possible to understand the reluctance of mesons to be captured into large angular momentum states in metals with small internuclear spacings on purely classical grounds. For a kaon to be captured into a state of $l = 100\hbar$ by an atom of radius 1 Å requires the kaon to have a minimum kinetic energy of ~ 50 eV. Thus, if the kaon succeeds in escaping localization upon a single atom until it has a lower energy than this, capture into large-l states would be quite unlikely. It should be pointed out that, even though there are many uncertainties in the calculations, several studies of the capture of slow negative mesons[6,10] have found that capture by a single atom occurs at energies somewhat in excess of this value.

It would certainly be beneficial to extend mesonic atom x-ray intensity measurements to other targets and other incident projectiles ($\bar{p}$, Σ^-, etc.). However, on the basis of the observations presented here, a study of the low-lying mesonic x-ray intensities in manganese or zinc in several of their crystalline forms should prove most interesting.

It is a pleasure to thank Professor Wiegand for a copy of his work before publication.

*Research supported, in part, by the U. S. Atomic Energy Commission, under Contract No. AT-(10-1)-3956.

[1]C. E. Wiegand and G. L. Godfrey, University of California, Lawrence Berkeley Laboratory Report No. LBL-1074, 1973 (to be published).

[2]D. Kessler, H. L. Anderson, M. S. Dixit, H. J. Evans, R. J. McKee, C. K. Hargrove, R. D. Barton, E. P. Hincks, and J. D. McAndrew, Phys. Rev. Lett. 18, 1179 (1967).

[3]D. Quitmann, R. Engfer, U. Hegel, P. Brix, G. Backenstoss, K. Goebel, and B. Stadler, Nucl. Phys. 51, 609 (1964).

[4]M. Leon and R. Seki, Phys. Rev. Lett. 32, 132 (1974).

[5]*American Institute of Physics Handbook*, edited by D. E. Gray (McGraw-Hill, New York, 1972), 3rd ed.

[6]A. D. Martin, Nuovo Cimento 27, 1359 (1963).

[7]Y. Eisenberg and D. Kessler, Phys. Rev. 130, 2352 (1963).

[8]J. R. Rook, Nucl. Phys. B20, 14 (1970).

[9]L. I. Ponomarev, Annu. Rev. Nucl. Sci. 23, 395 (1973).

[10]M. Y. Au-Yang and M. L. Cohen, Phys. Rev. 174, 468 (1963).

Resonant Enhancement of Two-Photon Absorption in Sodium Vapor

J. E. Bjorkholm and P. F. Liao
Bell Telephone Laboratories, Holmdel, New Jersey 07733
(Received 23 May 1974)

Resonant enhancement of over 7 orders of magnitude of the two-photon absorption cross section is observed in sodium vapor. Two cw dye-laser beams of different frequencies and propagating in opposite directions are utilized to generate high-resolution spectra which allow the enhancement as well as destructive-interference effects of nearly resonant intermediate states to be clearly demonstrated.

Recently there have appeared a number of papers demonstrating high-resolution two-photon spectroscopy in atomic vapors.[1,2] Especially interesting are the techniques which eliminate Doppler broadening by causing the atoms to absorb one photon from each of two beams of equal frequency propagating in opposite directions.[2] We have utilized a generalization of the opposing-beam technique to demonstrate resonant enhancement of the two-photon absorption cross section in sodium vapor. Our experiments were carried out using two single-mode, cw dye lasers operating at different frequencies. Large enhancements of more than 7 orders of magnitude and destructive-interference effects due to nearly resonant intermediate states are clearly demon-

strated.

The basic theory of two-photon absorption was given by Göppert-Mayer in 1931,[3] and since that time there has been considerable work on the theory of two-photon absorption in both solids and gases.[4] In the latter case calculations of two-photon photoionization[5] predicted strong enhancement of the photoionization cross section whenever a single photon energy approaches that of an allowed atomic transition. Destructive interference between the contributions from different intermediate states was also predicted. From second-order perturbation theory one can calculate the absorption cross section of an atom for light at frequency ν_1 induced by light at ν_2. The atomic transitions correspond to the atom absorbing one photon from each of the radiation fields. For linearly polarized light this induced-absorption cross section for transitions from the ground state g to the excited state f is given by

$$\sigma(\nu_1)=1.15\times10^{-34}\left|\sum_n\langle f|z|n\rangle\langle n|z|g\rangle[(E_n-h\nu_1)^{-1}+(E_n-h\nu_2)^{-1}]\right|^2\nu_1\rho(\nu_1+\nu_2)I_2\ \mathrm{cm}^2, \quad (1)$$

where I_2 is the intensity in W/cm^2 of the radiation field at ν_2, $\rho(\nu_1+\nu_2)$ is the normalized lineshape function for the transition, the matrix elements are expressed in Bohr radii, and the summation is carried out over all intermediate states of energy E_n, expressed in rydbergs. In our experiments we observe the $3S$-$4D$ transitions in sodium and the dominant intermediate states are the $3P$ levels. The induced cross section for this transition is approximately $(5\times10^{-14})I_2$ cm^2 when $E_{3P}-h\nu_2=0.1$ cm^{-1}. This can easily be made comparable to the single-photon absorption cross section per atom ($\lambda^2/4\pi$) of the strongly allowed $3S$-$3P$ resonance transition which is about 3×10^{-10} cm^2. Consequently it is not surprising that fluorescence caused by two-photon absorption was brightly visible in our experiments.

The basic experimental setup was straightforward. The light from two single-axial-mode, cw dye lasers propagated in opposite directions through a Pyrex cell containing sodium vapor. The beams were focused to a minimum beam radius in the vapor of about 40 μm and typical laser powers were 50 mW, so that maximum light intensities were about 10^3 W/cm^2. The vapor pressure was on the order of 10^{-5} Torr. Two-photon transitions to the $4D$ levels were monitored by using a 1P28 photomultiplier to detect the 330-nm fluorescence ($4P$-$3S$ transition) resulting from the decay from the $4D$ levels.

In making an experimental run, one laser was operated at a fixed frequency ν_2 while the other laser was operated at the frequency ν_1 which was electronically tuned across the two-photon transition. Because the frequencies of the two absorbed photons are not exactly equal, Doppler effects are not totally eliminated and the absorption linewidths contain residual Doppler broadening. Nonetheless, for the conditions of our experiments the observed linewidths (~60 MHz) are much smaller than the Doppler width (~3.4 GHz) and high-resolution spectra such as that shown in Fig. 1 were obtained. Calculations show[6] that the linewidth predicted for the conditions of Fig. 1 is 30 MHz; the experimentally observed linewidth (full width at half-maximum, FWHM) is 60 MHz. The increased linewidth is due to frequency jitter of the two lasers. The stability of the fixed-frequency laser was ± 35 MHz and that of the scanned laser[7] was about ± 10 MHz. (Note that for purposes of spectroscopy the 60-MHz linewidth of our experiment corresponds to a 30-MHz linewidth in the previous experiments[1,2] in which both photons were of the same frequency.) Averaging over seventeen curves like that of Fig. 1 we have measured the fine-structure splitting of the $4D$ state to be 1027 ± 16 MHz. This is in good agreement with previous measurements.[1]

The residual Doppler effects make it impossible to be resonant simultaneously with all velocity groups of the Maxwellian thermal distribution. Consequently the use of two photons of unequal frequencies results in a decrease of excitation efficiency. For the peaks of the lines, it

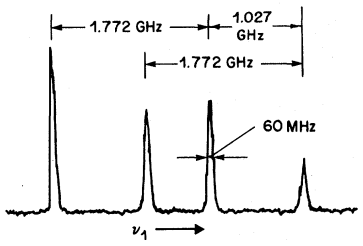

FIG. 1. The excitation spectrum for two-photon excitation of the $4D$ level with $\lambda_2=5835$ Å. Proceeding in the direction of higher frequency, the peaks correspond to the following transitions: $3S(F=2)\rightarrow4D_{5/2}$, $3S(F=2)\rightarrow4D_{3/2}$, $3S(F=1)\rightarrow4D_{5/2}$, $3S(F=1)\rightarrow4D_{3/2}$. The splittings 1.772 and 1.027 GHz correspond to the ground-state hyperfine splitting and our measurement of the $4D$ fine-structure splitting, respectively.

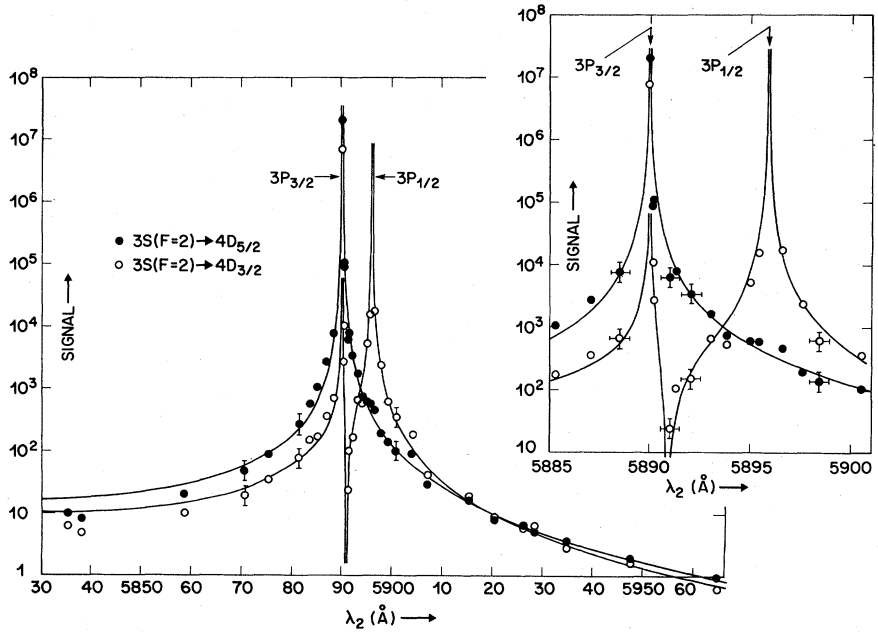

FIG. 2. Normalized two-photon transition rates for the $3S(F=2) \rightarrow 4D_{5/2}$ and $3S(F=2) \rightarrow 4D_{3/2}$ transitions as a function of the wavelength of the fixed-frequency laser, λ_2. (Note that $\nu_1 = \nu_2$ for $\lambda_2 = 5787$ Å.) The points are experimental and the curves are theoretical. The inset shows the behavior in the region from 5885 to 5900 Å with an expanded horizontal axis.

can be shown that the fraction η of atoms which can make two-photon transitions is given by[6]

$$\eta = ye^{y^2}\,\mathrm{erfc}(y). \qquad (2)$$

In the above, $y = (\ln 2)^{1/2}\nu_0/[\pi\tau\Delta\nu_D(\nu_1 - \nu_2)]$, where $h\nu_0$ is the energy of the $3S$-$4D$ transition ($\nu_0 = 1.036 \times 10^{15}$ Hz), τ is the natural lifetime of the excited state (52 nsec),[8] and $\Delta\nu_D$ is the Doppler width of the two-photon transition (~ 3.4 GHz). Over the tuning range used in our work η varied from 0.38 to 0.08. (The calculated linewidth varied from 30 to 100 MHz.)

To demonstrate resonant enhancement, a series of runs giving curves like that of Fig. 1 were carried out, each with a different λ_2, the wavelength of the fixed-frequency laser. In Fig. 2 we plot the normalized strengths of the $3S(F=2) \rightarrow 4D_{5/2}$ and $3S(F=2) \rightarrow 4D_{3/2}$ transitions as a function of λ_2. These normalized strengths were obtained by dividing the peak line strengths of each transition by the product of the incident laser powers. [The strengths of the transitions from the $3S(F=1)$ level to the two $4D$ levels are related to the respective transitions from the $3S(F=2)$ level by 0.6 and display the same behavior.] Recall that these lines are separated by much less than the Doppler width and that they could not be resolved without the use of the opposed-beam technique. For the point at the $3P_{3/2}$ resonance care was taken to attenuate the laser powers so that saturation effects such as line broadening were not present. Attenuation of about 10^3 was required. Saturation effects were not observed at all other points. Both transitions show strong dispersion as the laser frequency ν_2 approaches the frequency of the relevant $3P$ intermediate states. For the $3S(F=2) \rightarrow 4D_{5/2}$ transition only the $3P_{3/2}$ state can act as an intermediate state since the $3P_{1/2} \rightarrow 4D_{5/2}$ single-photon transition is forbidden, while for the $3S(F=2) \rightarrow 4D_{3/2}$ transition both the $3P_{3/2}$ and $3P_{1/2}$ levels are intermediate states. The wavelength dependence of the two-photon absorption cross section of the latter transition contains a sharp feature due to destructive interference between the contributions of the two intermediate levels for wavelengths lying between them. The cross section drops rapidly on the long-wavelength side of the $3P_{3/2}$ level and has a minimum only 1.00 Å from its maximum at the $3P_{3/2}$ level. The curves in Fig. 2 are theoretical curves calculated using Eqs. (1) and (2) where the sum in Eq. (1) has been restricted to the $3P$ levels. Except for an overall normalization factor, there are no adjustable param-

eters in this calculation. The relative amplitudes of all matrix elements were determined using angular momentum relations. The fit between experiment and theory is very satisfying. The slight discrepancy for the shortest wavelengths is due to the frequency jitter of the lasers. In this wavelength range the calculated absorption linewidth is comparable to or smaller than the total jitter.

In addition to the sharp two-photon signals, another feature was observed when the fixed-frequency laser was tuned close to one of the intermediate states. As the laser frequency ν_1 was scanned, this feature appeared at the frequency corresponding to $3P \rightarrow 4D$ transitions and was a broad resonance line with a width of about 1.9 GHz, the Doppler width for such transitions. Because the sum of the laser photon energies, $h\nu_1 + h\nu_2$, is not equal to the $3S \rightarrow 4D$ energy separation, we believe this signal is due to a two-step absorption process in which the first step involves direct excitation of $3S \rightarrow 3P$ transitions. This excitation requires a phase-interrupting collision simultaneous with the absorption of a photon, $h\nu_2$, to satisfy energy conservation. The second step consists of $3P \rightarrow 4D$ transitions. We are investigating this feature in more detail.

The large enhancements we have demonstrated clearly have important implications for potential applications of two-photon transitions. Such applications include selective two-photon excitation for isotope separation and the generation of sum and difference frequencies via three-wave mixing.[9]

We are pleased to acknowledge helpful discussions with M. D. Levenson of Harvard University and with A. Kiel, K. R. German, and J. P. Gordon of Bell Laboratories.

[1]D. Pritchard, J. Apt, and T. W. Ducas, Phys. Rev. Lett. 32, 641 (1974).

[2]F. Biraben, B. Cagnac, and G. Grynberg, Phys. Rev. Lett. 32, 643 (1974); M. D. Levenson and N. Bloembergen, Phys. Rev. Lett. 32, 645 (1974); N. Bloembergen, M. D. Levenson, and M. M. Salour, Phys. Rev. Lett. 32, 867 (1974); T. W. Hänsch, K. C. Harvey, G. Meisel, and A. L. Schawlow, to be published.

[3]M. Göppert-Mayer, Ann. Phys. (Leipzig) 9, 273 (1931).

[4]For a recent review see J. M. Worlock, *Laser Handbook*, edited by F. T. Arecchi and E. O. Schulz-DuBois (North-Holland, Amsterdam, 1972), p. 1323. For the theory of two-photon absorption without Doppler effects see L. S. Vasilenko, V. P. Chebotaev, and A. V. Shishaev, Pis'ma Zh. Eksp. Teor. Fiz. 12, 161 (1970) [JETP Lett. 12, 113 (1970)].

[5]W. Zernik, Phys. Rev. 135, A51 (1964); H. B. Bebb, Phys. Rev. 149, 25 (1966); J. L. Hall, IEEE J. Quantum Electron. 2, 361 (1966).

[6]J. E. Bjorkholm and P. F. Liao, to be published.

[7]Spectra-Physics System 580 dye laser.

[8]F. Karstensen and J. Schramm, Z. Phys. 195, 370 (1966).

[9]R. T. Hodgson, P. P. Sorokin, and J. J. Wynne, Phys. Rev. Lett. 32, 343 (1974); S. E. Harris and D. M. Bloom, Appl. Phys. Lett. 24, 229 (1974); D. M. Bloom, J. T. Yardley, J. F. Young, and S. E. Harris, Appl. Phys. Lett. 24, 427 (1974).

Advantages of a Nonharmonic-Oscillator Analysis of Molecular Vibrations*

Gary Simons
Department of Chemistry, Wichita State University, Wichita, Kansas 67208

and

J. Michael Finlan†
Department of Chemistry, The Johns Hopkins University, Baltimore, Maryland 21218

(Received 20 May 1974)

It is suggested that the theory of molecular vibrations, currently based on the harmonic oscillator potential, should be reformulated in terms of the potential $V = K[(x - x_e)/x]^2$. The proposed potential is shown to possess numerous advantages, including an improved physical form, superior eigenfunctions and eigenvalues, the ability to include rotation analytically, and a set of continuum wave functions. The standard classical vibrational analyses are retained.

The harmonic-oscillator potential,

$$V_{HO} = (K/2)[(x - x_e)/x_e]^2, \quad (1)$$

where x is a generalized coordinate with an equilibrium value of x_e, is widely used in the study of vibrations; indeed, this potential is so firmly entrenched that alternative analyses are rarely employed. Thus we find that the theory of molec-